International Journal of Terrestrial Heat Flow and Applied Geothermics
VOL. 4, NO. 1 (2021); P. 127-134.
ISSN: 2595-4180
DOI: https://doi.org/10.31214/ijthfa.v4i1.66

IJTHFA
http://ijthfa.com/

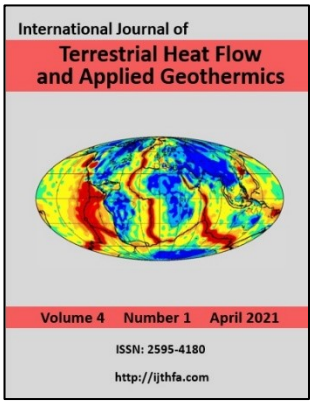

Keywords
Groundwater temperature,
Land use change,
Reforestation,
Growing season,
Climate proxy.

Received: January 29, 2020

Accepted: March 08, 2021

Published: April 01, 2021

Short- and long-term variations in groundwater temperature caused by changes in vegetation cover

Maria de Fatima Santos Pinheiro[1], Günther Buntebarth[2], Andrea Polle[3], Martin Sauter[1]

[1] Applied Geology, University of Göttingen, Göttingen, Germany.
[2] Institute of Geophysics, Clausthal University of Technology, Clausthal-Zellerfeld, Germany.
[3] Forest Botany and Tree Physiology, University of Göttingen, Göttingen, Germany.

Email address
guenter.buntebarth@tu-clausthal.de (G. Buntebarth)
Corresponding author

Abstract

Several comparative studies of the earth's surface provide evidence that vegetation and other bio-physical processes at the earth's surface can directly affect the atmospheric boundary layer, leading to changes in temperature and precipitation patterns. In this study, we demonstrate how vegetation cover can be responsible for the subsurface temperature variation as well as how this temperature variation can be related to past events. A linear decrease of 0.0407 K/year was estimated, and a decrease of 2 mK was observed in subsurface temperature when the surface temperature exceeded 9 °C. This diurnal temperature variation occurs during the phenological growing season of the vegetation. The transient temperature shows an annual cycle at a depth of 40 m. Model calculation applying a linear decrease in surface temperature of 2 K as a boundary condition was simulated. Comparing the results with the trend it is realistic to assume that when an apparent thermal diffusivity of $1.8*10^{-6}$ m²/s is applied an event starting between 10 and 20 years ago is responsible for the detected decrease in temperature. However, with this thermal diffusivity the conductive annual temperature variation reaches an amplitude of 1.1 mK instead of the measured 5.4 mK at 40 m. In conclusion, beside the vegetation causing additional convective heat transport triggered by the annual surface temperature, the influence of reduced solar incoming heat radiation reaching the ground caused by the increased shadowing effect of vegetation cover might be responsible for a continuous decrease in local temperature of 2 K being active approximately 20 years after plantation.

1. Introduction

The consequence of temperature changes at the Earth's surface as well as its penetration into the subsurface for the environment is of relevance today, especially with regard to the influence of the variation in vegetation cover. Understanding how it has changed through the years is important to predict future changes. The hydrological cycle is deeply affected by those changes, causing flood and drought around the world. One of the important forces in this cycle is transpiration. This process returns approximately 50% of precipitation to the atmosphere, and accounts for more than 60% of the evapotranspiration rate (Chahine, 1992; dos Santos et al., 2017; Good et al., 2015; Kumar et al., 2014; Schlesinger and Jasechko, 2014; Sun et al., 2011; Taiz et al., 2015).

The importance of transpiration for global climate as well as for crop growth is due to the fact that it links both hydrological and biological processes. The rate at which a crop transpires depends on several factors including atmospheric conditions, the shape and properties of the boundary between crop and atmosphere, root system distribution, soil hydraulic properties, and water availability. However, less than 5% of the water absorbed is retained by the plants (Chahine, 1992; dos Santos et al., 2017; Feddes et al., 2001; Prasad, 1988).

Several comparative studies of the earth's surface provide evidence that vegetation and other properties of the earth's surface can directly affect the atmospheric boundary layer, leading to changes in temperature and precipitation patterns (Beltrami and Kellman, 2003; Chahine, 1992; Griffiths et al., 2009; Zeppel et al., 2008). Such changes can also affect the dynamics of aquifer recharge, determined, among other

effects, by water infiltration into the soil and percolation of water through the unsaturated zone (Bense et al., 2013; Kordilla et al., 2012). In this study, we demonstrate how vegetation cover can affect subsurface temperature variations as well as provide information in how far this temperature variation can be related to past events.

1.1. Solar radiation and the vegetation cover

The distribution of the solar radiative energy flux between the surface and the atmosphere is controlled by the albedo of the Earth's surface. It affects many processes such as surface temperature and hydrological processes. Albedo varies with surface cover. On the one hand bright surfaces, such as deserts and snow, have a higher albedo, reflecting most of the incoming solar radiation. On the other hand, darker regions have a lower albedo, implying that the absorption of solar radiation is larger (Doughty et al., 2012; Wang et al., 2006).

Even though a decrease in albedo results in an increase in ground temperature, reforestation will result in a net cooling. The reason is that the structure of trees as well as the anatomy of leaves are specialized to increase the sunlight absorption. As a consequence, almost all of the photosynthetic photon flux density (PPFD) is absorbed by leaves before reaching the forest floor and it won't penetrate all the way to the bottom of the forest canopy. Moreover, compared to the variation in surface temperature, these areas will present a low temperature fluctuation in the soil (Berbet and Costa, 2003; Bodri and Cermak, 2011; Bright et al., 2017; Juang et al., 2007; Kaufmann et al., 2003; Taiz et al., 2015).

In addition, vegetation influences local and global energy balances important for the climate. The albedo in vegetated areas will vary seasonally with vegetation type as well as with location. Reason being that changes in vegetation cover modify not only albedo but also other important climate-driving variables, such as canopy height and rooting profile, which will affect surface roughness and evapotranspiration rates. Furthermore, crop productivity is directly related to the total amount of light received during the growing season, when it is considered that plants have both enough water and nutrients (Doughty et al., 2012; McElrone et al., 2013; Nepstad et al., 1994; Taiz et al., 2015).

1.2. Earth tides and transpiration rates

Recently, findings by Jahr et al. (2020) demonstrated the relationship between earth tide induced volume strain and changes in microtemperature. The authors related the change in microtemperature to the sub-vertical shift of the groundwater column, +/- parallel to the geothermal gradient, induced by fracture closure or dilation, depending on the magnitude of gravity forces. The effect of groundwater abstraction by vegetation particularly pronounced during growth phases of trees and shrubs, surrounding the monitoring borehole is highlighted as well.

In temperate climates, vegetation can be considered as a strong sink for soil water during the growing period, while only little water is consumed during the period of dormancy (Davi et al., 2006; Kramer, 2012). During the growth phase, water consumption fluctuates between day and night due to the light-driven opening of the stomata and consequently, results in diurnal variation of transpiration water loss (Davi et al., 2006; Dierschke, 1991; Schenker et al., 2014). The daily demand of water of a single, large tree can be several liters per square meter of ground surface to maintain plant water supply. Some species grow roots to depths of several tens of meters. Roots of trees exhibit a negative pressure difference compared to the matric potential of the soil at shallow depths, inducing water flow by the root system. Similarly, with shallow groundwater tables, the abstraction of groundwater by trees can be described by the radial flow equation, based on Darcy's law, with the flow rate being determined by the hydraulic potential gradient and the hydraulic conductivity of the soil and/or fractured rock system. Moreover, a tidal rhythm has been observed in plants both in an open site and in a controlled environment (Holzknecht and Zürcher, 2006; Zürcher et al., 1998).

In the fractured rock aquifer of the Göttingen North-Campus, fluid flow is believed to be initiated by a change in hydraulic potential, e.g. ambient groundwater flow or groundwater abstraction, or by a change in fracture aperture following a change in volume strain. Both types of mechanisms result in a temperature variation assuming a steady state geothermal heat flux from the centre of the earth and a (sub-)vertical displacement of the groundwater column.

The effect of heat conduction following surface temperature changes is small. Early studies of Muncke (1827) led to an analytical solution of the heat conduction equation for a temperature wave penetrating into the subsurface. Already in 1837, Lambert-Adolphe-Jacques Quetelet (1796-1874) described the diurnal and annual temperature variations as sine waves (Buntebarth, 2002). Applying the conductive heat conductance, daily temperature variations are attenuated to 0.001 K at a depth of ca. 1.5 m and annual changes reach the same amplitude at ca. 30 m assuming a mean thermal diffusivity of 1 mm²/s and a surface temperature amplitude of ± 10 K (Buntebarth et al., 2019). These calculations demonstrate the effect of pure conductive heat flow.

The effect of free convective flow due to vertical temperature differences in the observation borehole can be neglected as well, as discussed below.

2. Methodology

2.1. Study area

Figure 1 - Satellite images of the area of investigation of the years 1999 (A) and 2016 (B) by Stadt Göttingen.

The city of Göttingen is located in the Leinetal graben, part the West European rift zones. The geology of this area, as well as the profile of the borehole is detailed by Buntebarth and collaborators (Buntebarth et al., 2019). From previous works in the study area, it is assumed that the thermal diffusivity ranges from 0.8 to $1.1*10^{-6}$ m^2/s (Baetzel, 2017). At present

the area is characterized by high scrubland and approx. 20 m high maple and birch trees, which grow at distances between 15 and 25 m to the boreholes (Figure 1B). In this image, the five-spot borehole configuration is visible. The first well of the arrangement was drilled in 2008, and the other four, including the Northern well, equipped with the thermal sensors, were drilled in 2012. Compared to the satellite image of 1999 (Figure 1A) an increase in the vegetation cover can be observed. The trees were most likely planted during the period 1980-1985. In 1999 a shed was constructed in the center of the area and a pond was excavated to the east for fire protection purposes. Previously this region of Göttingen was clear.

2.2. The analytical heat conduction model

The subsurface temperature variations can be spectrally decomposed into thermal disturbances of different periods, with varying amplitudes and phase relationships. For that reason, the thermal temperature profile can reveal information from past climate events. It occurs because, according to the theory of heat conduction, changes in surface temperature propagate downward as thermal waves or perturbations, with amplitudes decreasing exponentially with depth. Moreover, the rate of propagation of the thermal signal is governed mainly by thermal diffusivity, which is directly proportional to the thermal conductivity of the material. Due to this, temperature changes on the earth's surface propagate slowly downwards, as a consequence of the relatively low thermal diffusivity of rocks (Bodri and Cermak, 2011; Carslaw and Jaeger, 1992; Cermak, 1971; Hamza and Vieira, 2011; Harris and Chapman, 1997; Majorowicz and Safanda, 2005; Pollack and Huang, 2000; Smerdon et al., 2003; Tautz, 1971).

Furthermore, the attenuation during propagation depends on the frequency of the waves. Waves with longer periods of time, such as a long-term temperature variation, will have less attenuation, propagating to larger depths compared to short-term temperature variations. Signs of regional climate change may be, however, overshadowed by changes in anthropogenic activity that affect land use or vegetation patterns. For that reason, other possible sources of temperature perturbations must be considered (Cermak and Bodri, 2018; Demetrescu and Shimamura, 1997; Middleton, 1999; Pimentel and Hamza, 2013; Prensky, 1992).

The penetration of a thermal signal into the subsurface can be calculated in space and time by simple heat conduction models. For this purpose, the steady state background temperatures associated with deep heat flow should be separated. The remaining temperature profile after separation (residual temperature) contains the components of the original observations considered as transient. This transient component, when analyzed, produces a reconstruction of the climatic variations in the surface. By solving the equation of heat conduction with temperature steps as a boundary condition, it can be checked whether any event in the past may have resulted in a spontaneous change in temperature as it occurs after deforestation (Bodri and Cermak, 2011; Carslaw and Jaeger, 1992; Cermak, 1971; Nitoiu and Beltrami, 2005; Tautz, 1971).

$$T(z,t) = \pm T_0\left(1 - erf\left(\frac{z}{2\sqrt{(at)}}\right)\right) \quad (1)$$

T corresponds to the temperature at depth z in a time t with the thermal diffusivity α and the temporal derivative as:

$$\left(\frac{\partial T}{\partial t}\right)_{z=const} = \pm T_0 \frac{z}{2\sqrt{(\pi a t^3)}} \exp\left(\frac{-z^2}{4at}\right) \quad (2)$$

The application of a continuous surface temperature increase or decrease (±T_0) in a specific time in the past (k) as boundary condition can simulate, however, previous events of surface temperature variation.

$$T(z,t) = \pm T_0 \frac{z^2}{ka}\left[\left(\frac{at}{z^2} + \frac{1}{2}\right) erfc\left(\frac{z}{2\sqrt{(at)}}\right) - \frac{1}{\sqrt{(\pi)}}\sqrt{\left(\frac{at}{z^2}\right)} \exp\left(\frac{-z^2}{4at}\right)\right] \quad (3)$$

With the temporal derivative as:

$$\left(\frac{\partial T}{\partial t}\right)_{z=const} = \pm T_0 \frac{1}{k} erfc\left(\frac{z}{2\sqrt{(at)}}\right) \quad (4)$$

2.3. Measurements

Today's technological advance in the measurement of the groundwater temperature allows to monitor changes in temperature at very high resolution, in the range below Millikelvins. Here, the LogBox microT temperature recording equipment will be used for long-term monitoring of temperatures at the selected depths, a high precision thermometer with a resolution of 0.0002 degrees (www.geotec-instruments.com). The instrument is protected by a waterproof housing and is directly located in the metal protected well head. A waterproof stainless-steel housing protects the calibrated temperature sensor fixed at the depths of 40 m and 78 m. The temperature sensitivity is related to the variation of the resonance frequency ($\Delta f(T)/f_0$) of the quartz sensor. Its linearized sensitivity which can be applied within a limited temperature variation (T-25) is: $\Delta f(T)/f_0 = -3*10^{-5}$ (T-25) according to the datasheet of the MicroCrystal sensor MX2T. A temperature compensated frequency counter determines the sensor frequency which must be processed for evaluation of the temperature.

3. Results

Long-term temperature measurements were conducted during the period October 2016 to September 2018 at the depths of 40 and 78 m. The greater depth of 78 m might be less influenced by groundwater abstraction by trees and is used for comparison. Based on these measurements, 6 graphs were plotted. Daily mean values are plotted in Figure 2. The daily average temperature at depth of 40 m shows a continuous decrease, from 11.0091 °C in October 2016 to 10.9258 in September 2018. The annual temperature variation of 0.0407 K/year is observed when a linear trend is applied. The decrease in temperature can be explained by the increased shadowing effect of the growing vegetation cover, decreasing both the local air temperature and the solar radiation reaching the ground.

Comparing temperature records at depths of 40 m with those at 78 m depth, it is possible to extract the raw data series showing different temperature drifts depending on the recording depth. A total increase of 0.04 K at 78 m and a decrease of 0.1 K at 40 m is recorded. The linear trend shows a temperature rise of 0.01 K/year at 78 m and a decrease of 0.02 K/year at 40 m. Applying Equation 4 and assuming a

continuous surface temperature increase of 2 K for the last 100 years, an increase of 0.01 K/year in temperature at 78 m can only be observed in 100 years from now. However, if a thermal diffusivity of $1.8*10^{-6}$ m^2/s is applied, a continuous increase occurring for the last 100 years in the past is realistic.

Periodical variations occur at both depths, but they can be attributed to different types of mechanisms. At larger depths, different types of processes contribute to temperature variations, e.g. hydrological and earth tidal processes, demonstrated by (Jahr et al., 2020).

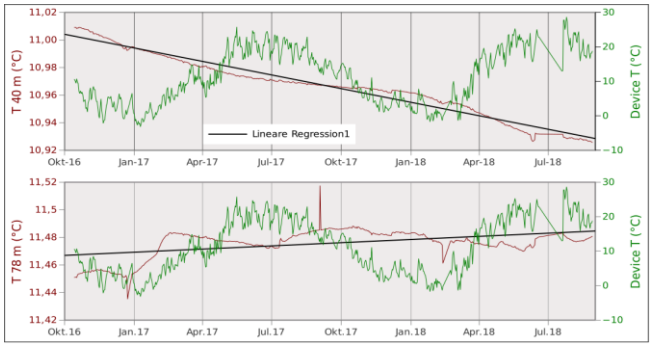

Figure 2 - Daily average temperatures at depths of 40 and 78 m as well as the device temperature at the field site of the Göttingen North-Campus between October 2016 and September 2018. The black line represents the linear trend of the temperature at both depths.

Comparing the daily temperature sequence at the depth of 40 m and at the surface in March 2017 and March 2018 (Figure 3) a decrease in subsurface temperature can be observed when the surface temperature reaches a value of nearly 9 °C. As concluded before (Buntebarth et al., 2019), a diurnal temperature variation of approximately 2 mK occurs during the phenological growing season of the vegetation. The increase in surface temperature during spring is responsible for the end of the dormant vegetation period. It results in an increase of water abstraction by plants. Observing the daily temperature sequence at 78 m during March 2017 (Figure 4) it can be noticed that at 78 m depth, as well as at 40 m depth, a relation with the surface temperature variation exists.

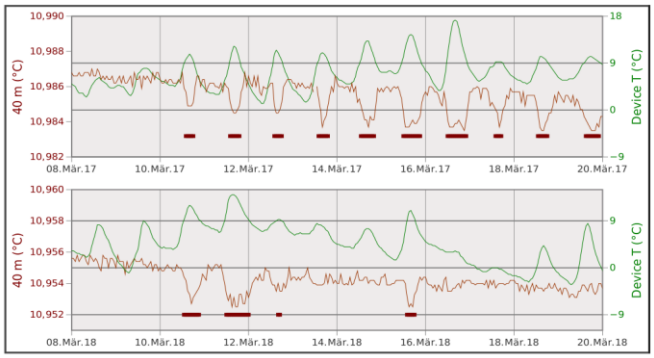

Figure 3 - Comparison between daily temperature sequence at 40 m depth and at the surface in both March 2017 and 2018. Solid thick lines illustrate time periods of T >9 °C.

Apart from the relationship between surface and subsurface temperature variations, the periodical variations can also partly be explained by the influence of earth tides (Buntebarth et al., 2019; Jahr et al., 2020) inducing fluid flow variations at daily and half-daily periods. This fluid flow can be explained by changes in volume strain, i.e. opening and closing fractures of the rock mass resulting from changes in gravitational forces of the sun and moon. Consequential variations in porosity and permeability induce fluid flow.

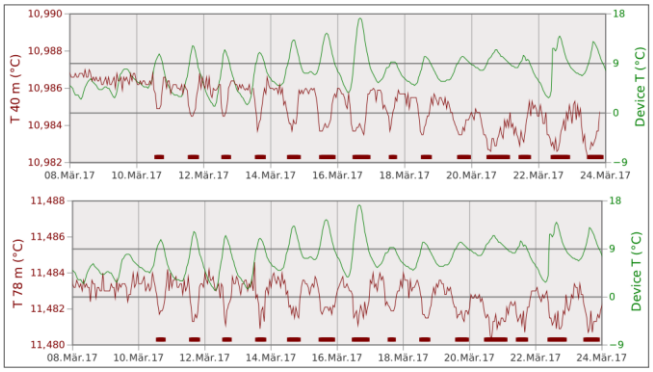

Figure 4 - Comparison between daily temperature sequence at 40 and 78 m depths and at the surface March 2017. Solid thick lines time periods of T >9 °C.

The constant heat flow from the earth's interior which results in a linear temperature increase with depth, i.e. a constant geothermal gradient, is superposed by the transient heat flux component resulting from the above tidally induced fluid flow. Since most fractures are characterized by a sub-vertical geometry, the above fluid flow has a major vertical flow component and therefore contributes to temperature variations at a fixed depth, i.e. at the level of the borehole temperature sensor.

The main contribution to the change in gravitational force can be attributed to the moon. Its magnitude and the resulting volume strain in the subsurface are determined mainly by the moon phase. Figure 5 demonstrates that the temperature amplitudes are generally larger during days of syzygy, i.e. approximately during times of maximal gravitational force, and lower during times of minimal gravitational force (half-moon). This coincidence between temperature variations and the theoretical changing volume strain is apparent in both temperature records, i.e. at 40 and 78 m depths (Jahr et al., 2020).

The relationship between volume strain and temperature at 40 m depth is visualized in Figure 6. The theoretical volume strain at the borehole location coincides, in general, with the amplitude of the recorded temperature. During the time period studied the temperature record in Figure 5 is superimposed by a decreasing trend. In addition to the volume strain, the moon phases are shown in Figure 6, departing slightly from the corresponding minima and maxima of volume strain. This deviation can be attributed to the complex change in moon-sun-earth gravitational forces (Jahr et al., 2020). The close relationship between the respective moon phase and the magnitude of the temperature amplitude is apparent except for a few days at the beginning of May 2017.

While during April hardly any precipitation was recorded, an intensive storm event with 23.3 mm of rainfall was measured at the location during the time period of 4. – 5. May 2017. With the availability of sufficient water close to the surface the trees and shrubs did not abstract groundwater from the aquifer, with the consequence of considerably reduced temperature amplitudes. The time of half-moon on May 18 did not coincide with the minimum of volume strain so that the amplitude of temperature change decreased a few days later at the strain minimum.

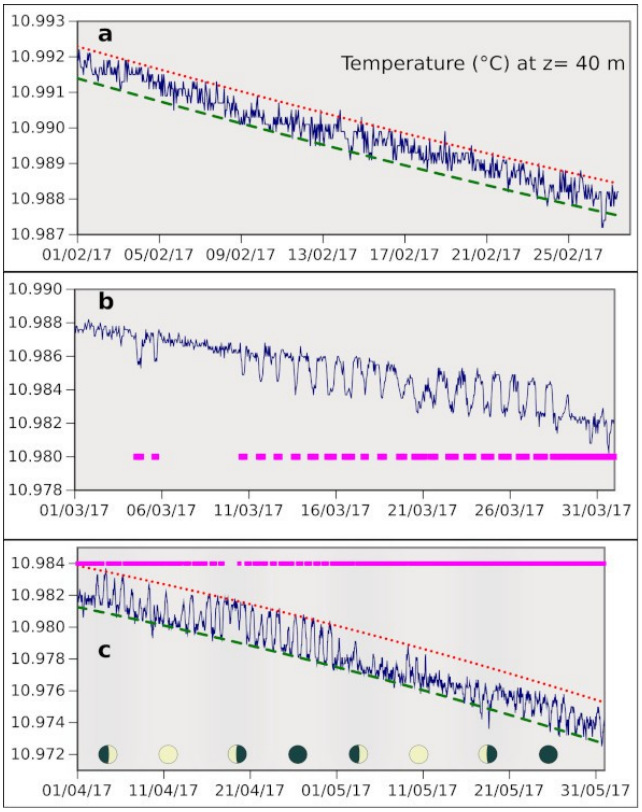

Figure 5 - Temperature variations at z= 40 m between winter 2016 and during spring 2017; a) Temperature record during February 2017 with upper (dotted red) and lower (dashed green) limit; the surface temperatures are below T= 9 °C; b) Temperature record with increased amplitudes at days with surface temperatures higher than T= 9 °C (Broken solid pink line illustrates time periods of T>9°C and time periods of T<9°C (blank)); c) Temperature record with upper (dotted red) and lower (dashed green) limit and surface temperatures higher than T= 9 °C. Broken solid pink lines illustrate time periods of T>9°C (solid pink) and time periods of T<9°C (blank) and the moon phase during spring 2017.

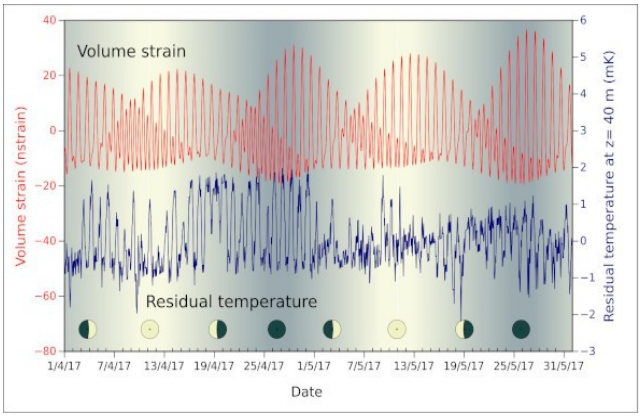

Figure 6 - Theoretical volume changes (Nano strain) with moon phase and the residual temperature at z= 40 m, i.e. recorded temperature corrected for trend.

Highest temperature variations, i.e., daily and half daily variations, are mainly observed during spring and relate to the moon phases and times of growing vegetation. This phenomenon is also recognized during the years 2016 and 2018 (Buntebarth et al., 2019). However, the daily and half-daily temperature periods with the change in the moon phases are not apparent during summer and autumn which leads to the conclusion that the trees abstract only small volumes of groundwater during these times.

By separating the residual values from the linear trend to the measured data, it is possible to observe both the steady state background temperature and the transient component.

In Figure 7a, the transient component is compared with the surface temperature. At the ground surface the temperature amplitude observed was approximately 12 ˚C while at a depth of 40 m the amplitude of the residual temperature was measured at approximately 0.007 ˚C. The theoretical heat conduction effect is also presented. In Figure 7b, the effect of heat conduction was added to the residual temperature. As a consequence, the slope was slightly changed. The transient temperature coincides in phases at the depth of 40 m, showing a phase shift of ca. half a year. It was also observed that the water absorption by trees achieved its maximum ca. 40 days before the maximum of the surface temperature. Furthermore, the slight difference to the annual cycle is an indication that the maximum water consumption occurs before the annual temperature maximum. Interruption of records and reinstallation generated an offset of ca. 2 mK in 2018.

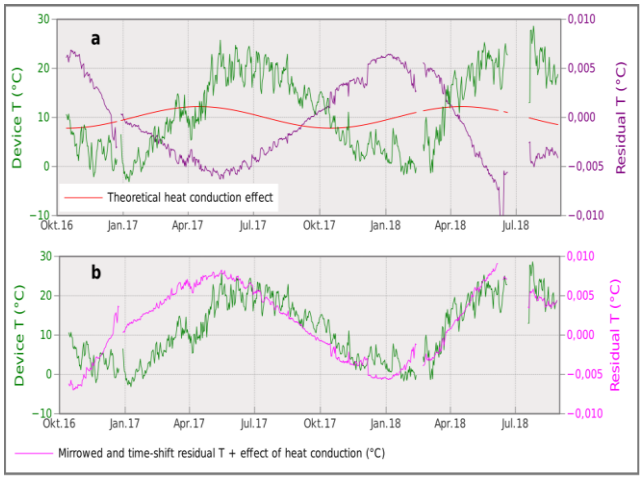

Figure 7 - a) Comparison between the device temperature and the residual temperature at depth of 40 m. The red line corresponds to the theoretical heat conduction effect; b) The magenta line corresponds to the mirrored and time shifted residual temperature at depth of 40 m with the included effect of heat conduction. The graph above represents the phase shift of the residual values of 183 days.

This observation can be explained by the activity of vegetation being intensified during spring and summer, when the water potential in plants increases. As a result, the residual temperature of the groundwater decreases. In contrast, when the surface temperature decreases and the vegetation enters into a dormant period, the residual temperature at 40 m depth increases.

Between October and December 2016, the residual value was expected to be higher than that measured. The difference shows an apparent increase in vegetation activity prior to the period expected. The amplitude temperature variation at the surface might have affected vegetation activity during autumnal senescence.

In contrast to a sudden deforestation, accompanied by a spontaneous change in surface temperature, reforestation can be described as a gradual, continuous surface temperature decrease. Considering a continuous decrease in surface temperature of 2 K as a boundary condition, equivalent to the reported temperature step expected after deforestation, equation 4 can be applied. Figure 8 shows the simulation of an event starting between 10 and 30 years ago (from 1990 to

2010), i.e. the time period of the area of the increasing tree canopy. Considering the expected thermal diffusivity ($1.0*10^{-6}$ m^2/s) the change in temperature would only be observed in a few years from now. However, when a thermal diffusivity of $1.8*10^{-6}$ m^2/s is assumed, a continuous decrease in temperature from 10 to 20 years ago is realistic.

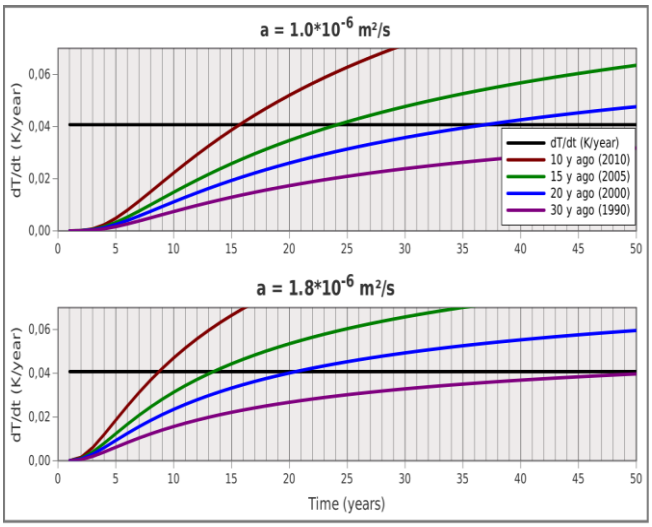

Figure 8 - Temperature changes with elapsed time at the depth of 40 m after a continuous temperature change starting 10, 15, 20 and 30 years ago. The black line represents the present linear trend of the temperature variation at the depth of 40 m.

4. Discussion and conclusion

Subsurface temperature changes can be the effect of a multitude of processes, i.e., the change in surface temperature, convective and conductive geothermal heat flow, hydrological and hydrogeological processes as well as the above discussed crustal deformation and abstraction by vegetation.

The observed microtemperature variations at the Göttingen North-Campus site are suggested to be the result of the superposition of the effects of two main processes and several other factors: The dominating processes are: a) the displacement of the fluid column parallel to the geothermal gradient by earth tide enforced opening and closing of rock fractures, and b) the abstraction of groundwater by the root network of deciduous trees and shrubs. The effects of borehole heat advection, heat conduction from surface temperature variations is negligible and ambient groundwater flow only occurs at shallow depths where considerably higher hydraulic conductivity prevails.

The surface temperature variation signal is attenuated, and phase-shifted with depth and is characterized by an amplitude of 1 mK and a phase shift of 1.5 years at a depth of 40 m, with an apparent thermal diffusivity applied resulting from the effect of the growing vegetation. Frequently, in an environment with high geothermal gradients, the effect of free convection in a borehole is believed to contribute to vertical flow as well, possibly superimposing flow induced by earth tides and abstraction by vegetation. Luheshi (1983) estimated the minimum temperature gradient in a borehole at 8.5 in. diameter for convection driven flow to occur at 0.06 K/m. At the experimental site in Göttingen the borehole diameter is 15.24 mm (6 in) only and the geothermal gradient amounts to ca. 0.015 K/m (Buntebarth et al., 2019), i.e. below the critical threshold for free convection.

In our study, we recorded temperature fluctuations that reflect changes in groundwater flow with distinct daily and seasonal patterns. Looking at short-term variations it could be observed that daily as well as annual temperature variations are influenced by fluid flow, i.e. convective heat transport induced by plant activities, and in contrast to heat conduction theory, this variation can be observed at larger depths. During spring and summer, temperature fluctuations can be explained by diurnal changes in water consumption of vegetation, which increases during the day and decreases at night.

Mature, large trees such as the maple trees close to the borehole consume up to several hundreds of litres of water per day. For example, Pisek and Tranquillini (1951) found that ca. 14 m tall conifers transpired between 80 and 180 l of water per day. Water consumption starts in March and remains high until October. Deciduous tree species exhibit generally larger transpiration rates compared to other species. For beech trees, up to 500 l per day have been reported (https://www.ds.mpg.de/139253/05). However, their seasonal water demand is delayed compared to that of coniferous trees because their above-ground growth activity starts in April and May (Dierschke, 1991). In contrast to the above-ground physiology, root growth starts much earlier, when soil temperatures range slightly above the freezing point (Gaul et al., 2008; Hansen et al., 1996). For maple trees, minimum temperature for root growth is 3 °C (Schenker et al., 2014).

However, at low surface temperatures, vegetation growth activity is considerably reduced. Correspondingly, root water uptake depends largely on temperature. Soil temperatures below 5 to 7 °C inhibit water uptake by herbs and trees because of higher water viscosity and lower membrane permeability (Leuschner and Ellenberg, 2017). Our data agree with this threshold considering that residual values of temperature at 40 m depth reached a minimum, when environmental temperatures ranged around 9 °C.

Although roots of some species can reach deep soil layers of up to 10 or 20 m, they do not grow to depths of 40 m. The abstraction of groundwater by plants can be visualized similarly to that of the flow configuration close to a partially penetrating abstraction well, i.e. with considerable vertical flow components. In such type of wells, the hydraulic potential is lowered at shallow depths, inducing fluid flow to the well screen not only as radial horizontal component but also as vertical flow from larger or shallower depths depending on the subsurface geo-hydraulic characteristics and precipitation.

In addition, the periodically changing gravitational forces cause changes in poro-perm rock properties depending on the sun/moon geometric configuration. The continuous change in volume strain causes alternating dilation or closure of subsurface fractures inducing changes in the geometry of flow paths and the magnitude of fluid flux and therefore heat flow. During times of maximum strain, the rock fracture apertures are increased, and groundwater flow is enhanced compared to those periods of minimum strain. The vertical displacement of the fluid column is estimated at ca. 0.18 m based on a geothermal temperature gradient of $\Delta T/\Delta z$ = 0.0135 K/m (Buntebarth et al., 2019) and a maximum amplitude of ΔT= 2.5 mK.

When the long-term variation is taken into account, vegetation again plays an important role. Changes in vegetation cover will influence not only climate itself, being responsible for i.e. surface temperature variation and precipitation patterns, but also for both changes in distribution

of solar radiation and changes in soil layer. Even though vegetation is known to decrease the albedo of the area, radiation will not be absorbed by the soil, but by the plants. As a consequence, the subsurface temperature will decrease.

In this study, with the only variation in land use being the growth of trees around the borehole, the long-term influence starts not at the time the trees were planted (35-40 years ago), but at the time the vegetation cover became of relevance to the albedo (10-20 years ago).

Here, thermal diffusivity is evaluated at a value higher than the expected. The abstraction of water by the roots in shallow layers might be the reason for the additional temperature decrease at 40 m. Additionally, it is important to point out that an increase in vegetation cover might be responsible for a decrease in local temperature of 2 K, expected to have an influence approximately 20 years after plantation. Furthermore, global warming of 2 K in 100 years would have a much lower rate of warming compared to the effect of vegetation described above.

Finally, with the technological advance in groundwater temperature measurements, changes in groundwater temperature seems to be a promising method to understand climate variation as well as the potential impacts of land use change. Currently we are developing a numerical model simulating the hydromechanically controlled heat transport of the fractured rock mass, integrating also the effect of groundwater abstraction by vegetation. This model will allow us to investigate the relative importance of the different drivers and system characteristics.

Acknowledgments

The authors would like to thank all technicians involved in the installation and maintenance of the instruments at the borehole array in Göttingen, in particular Steffen Fischer and Dr. Thomas Jahr, Institut für Geowissenschaften der Friedrich-Schiller-Universität, Jena/Germany for calculating the earth tides of the borehole location. We are also grateful to the anonymous reviewers who provided many helpful corrections to improve the manuscript.

References

Baetzel, K. 2017. Hydrogeological Characterization of a fractured aquifer based on Modelling and Heat Tracer Experiments. (Unpublished Master Thesis). University of Göttingen,

Beltrami, H., Kellman, L. 2003. An examination of short- and long-term air–ground temperature coupling. Global and Planetary Change, 38(3-4), 291-303. DOI 10.1016/s0921-8181(03)00112-7

Bense, V. F., Gleeson, T., Loveless, S. E., Bour, O., Scibek, J. 2013. Fault zone hydrogeology. Earth-Science Reviews, 127, 171-192. DOI 10.1016/j.earscirev.2013.09.008

Berbet, M.L., Costa, M.H. 2003. Climate change after tropical deforestation: seasonal variability of surface albedo and its effects on precipitation change. Journal of Climate, 16(12), 2099-2104.

Bodri, L., Cermak, V. 2011. Borehole climatology: a new method how to reconstruct climate: Elsevier.

Bright, R.M., Davin, E., O'Halloran, T., Pongratz, J., Zhao, K., Cescatti, A. 2017. Local temperature response to land cover and management change driven by non-radiative processes. Nature Climate Change, 7(4), 296-302.

Buntebarth, G. 2002. Temperature measurements below the Earth's surface: A history of records. Earth sciences history, 21(2), 190-198.

Buntebarth, G., Pinheiro, M., Sauter, M. 2019. About the penetration of the diurnal and annual temperature variation into the subsurface. International Journal of Terrestrial Heat Flow and Applied Geothermics, 2(1), 1-5.

Carslaw, H.S., Jaeger, J.C. 1992. Conduction of heat in solids: Claredon Press.

Cermak, V. 1971. Underground temperature and inferred climatic temperature of the past millenium. Palaeogeography, Palaeoclimatology, Palaeoecology, 10, 1-19.

Cermak, V., Bodri, L. 2018. Attribution of precipitation changes on ground–air temperature offset: Granger causality analysis. International Journal of Earth Sciences, 107(1), 145-152.

Chahine, M.T. 1992. The hydrological cycle and its influence on climate. Nature, 359, 373-380.

Davi, H., Dufrêne, E., Francois, C., Le Maire, G., Loustau, D., Bosc, A., Moors, E. 2006. Sensitivity of water and carbon fluxes to climate changes from 1960 to 2100 in European forest ecosystems. Agricultural and Forest Meteorology, 141(1), 35-56.

Demetrescu, C., Shimamura, H. 1997. Groundwater microtemperature measurements in Romania, 142-146, in: Buntebarth, G. Microtemperature Signals of the Earth's Crust. Paper presented at the 5th International Congress of the Brazilian Geophysical Society.

Dierschke, H. 1991. Phytophänologische Untersuchungen in Wäldern: Methodische Grundlagen und Anwendungsmöglichkeiten im passiven Biomonitoring. Veröff. Natursch. u. Landschaftspfl. Bad.-Württemb., Beih, 64, 76-86.

dos Santos, M.A., de Jong van Lier, Q., van Dam, J.C., Freire Bezerra, A.H. 2017. Benchmarking test of empirical root water uptake models. Hydrology and Earth System Sciences, 21(1), 473-493. DOI 10.5194/hess-21-473-2017

Doughty, C.E., Loarie, S.R., Field, C.B. 2012. Theoretical Impact of Changing Albedo on Precipitation at the Southernmost Boundary of the ITCZ in South America. Earth Interactions, 16(8), 1-14. DOI 10.1175/2012ei422.1

Feddes, R.A., Hoff, H., Bruen, M., Dawson, T., Rosnay, P., Dirmeyer, P., Pitman, A.J. 2001. Modeling Root Water Uptake in Hydrological and Climate Models. Bulletin of the American Meteorological Society, 82(12), 2797-2810.

Gaul, D., Hertel, D., Leuschner, C. 2008. Effects of experimental soil frost on the fine-root system of mature Norway spruce. Journal of Plant Nutrition and Soil Science, 171(5), 690-698.

Good, S.P., Noone, D., Bowen, G. 2015. Hydrologic connectivity constrains partitioning of global terrestrial water fluxes. Science, 349(6244), 175-177.

Griffiths, R.P., Madritch, M.D., Swanson, A.K. 2009. The effects of topography on forest soil characteristics in the Oregon Cascade Mountains (USA): Implications

for the effects of climate change on soil properties. Forest Ecology and Management, 257(1), 1-7. DOI 10.1016/j.foreco.2008.08.010

Hamza, V.M., Vieira, F.P. 2011. Climate Changes of the Recent Past in the South American Continent: Inferences Based on Analysis of Borehole Temperature Profiles. Climate Change – Geophysical Foundations and Ecological Effects, 113-136.

Hansen, J., Vogg, G., Beck, E. 1996. Assimilation, allocation and utilization of carbon by 3-year-old Scots pine (Pinus sylvestris L.) trees during winter and early spring. Trees, 11(2), 83-90.

Harris, R.N., Chapman, D.S. 1997. Borehole temperatures and a baseline for 20th-century global warming estimates. Science, 275, 1618-1621.

Holzknecht, K., Zürcher, E. 2006. Tree stems and tides–A new approach and elements of reflexion (reviewed paper). Schweizerische Zeitschrift fur Forstwesen, 157(6), 185-190.

Jahr, T., Buntebarth, G., Sauter, M. 2020. Earth tides as revealed by micro-temperature measurements in the subsurface. Journal of Geodynamics, 136, 101718.

Juang, J. Y., Katul, G., Siqueira, M., Stoy, P., Novick, K. 2007. Separating the effects of albedo from eco-physiological changes on surface temperature along a successional chronosequence in the southeastern United States. Geophysical Research Letters, 34(21).

Kaufmann, R., Zhou, L., Myneni, R., Tucker, C., Slayback, D., Shabanov, N., Pinzon, J. 2003. The effect of vegetation on surface temperature: A statistical analysis of NDVI and climate data. Geophysical Research Letters, 30(22).

Kordilla, J., Sauter, M., Reimann, T., Geyer, T. 2012. Simulation of saturated and unsaturated flow in karst systems at catchment scale using a double continuum approach. Hydrology and Earth System Sciences Discussions, 9(2), 1515-1546. DOI 10.5194/hessd-9-1515-2012

Kramer, P. 2012. Physiology of woody plants: Elsevier.

Kumar, R., Shankar, V., Jat, M.K. 2014. Evaluation of root water uptake models – a review. ISH Journal of Hydraulic Engineering, 21(2), 115-124. DOI 10.1080/09715010.2014.981955

Leuschner, C., Ellenberg, H. 2017. Ecology of central European forests: Vegetation ecology of Central Europe, volume I (Vol. 1): Springer.

Majorowicz, J., Safanda, J. 2005. Measured versus simulated transients of temperature logs—a test of borehole climatology. Journal of Geophysics and Engineering, 2(4), 291-298. DOI 10.1088/1742-2132/2/4/s01

McElrone, A.J., Choat, B., Gambetta, G.A., Brodersen, C.R. 2013. Water uptake and transport in vascular plants. Nature Education Knowledge, 4(6).

Middleton, M. 1999. Modelling of temperature disturbances due to groundwater flow associated with seismic activity, 93-103. Microtemperature signals of the Earth's crust.

Muncke, G.W. 1827. Gehlers physikalisches Wörterbuch. Leipzig: EB Schwickert, 3, 970-1068.

Nepstad, D.C., de Carvalho, C.R., Davidson, E.A., Jipp, P.H., Lefebvre, P.A., Negreiros, G.H., . Vieira, S. 1994. The role of deep roots in the hydrological and carbon cycles of Amazonian forests and pastures. Nature, 372(6507), 666-669. DOI 10.1038/372666a0

Nitoiu, D., Beltrami, H. 2005. Subsurface thermal effects of land use changes. Journal of Geophysical Research, 110(F1). DOI 10.1029/2004jf000151

Pimentel, E.T., Hamza, V.M. 2013. Use of geothermal methods in outlining deep groundwater flow systems in Paleozoic interior basins of Brazil. Hydrogeology Journal, 22(1), 107-128. DOI 10.1007/s10040-013-1074-0

Pisek, A., Tranquillini, W. 1951. Transpiration und Wasserhaushalt der Fichte (Picea excelsa) bei zunehmender Luft-und Bodentrockenheit. Physiologia Plantarum, 4(1), 1-27.

Pollack, H.N., Huang, S. 2000. Climate Reconstruction from Subsurface Temperatures. Annual Review of Earth and Planetary Sciences, 28(1), 339-365. DOI 10.1146/annurev.earth.28.1.339

Prasad, R. 1988. A linear root water uptake model. Journal of Hydrology, 99, 297-306.

Prensky, S. 1992. Temperature Measurements in Boreholes: An Overview of Engineering and Scientific Applications. The Log Analyst, 33(03), 313-333.

Schenker, G., Lenz, A., Körner, C., Hoch, G. 2014. Physiological minimum temperatures for root growth in seven common European broad-leaved tree species. Tree physiology, 34(3), 302-313.

Schlesinger, W.H., Jasechko, S. 2014. Transpiration in the global water cycle. Agricultural and Forest Meteorology, 189-190, 115-117. DOI 10.1016/j.agrformet.2014.01.011

Smerdon, J.E., Pollack, H.N., Enz, J.W., Lewis, M.J. 2003. Conduction-dominated heat transport of the annual temperature signal in soil. Journal of Geophysical Research: Solid Earth, 108(B9). DOI 10.1029/2002jb002351

Sun, G., Alstad, K., Chen, J., Chen, S., Ford, C. R., Lin, G., Zhang, Z. 2011. A general predictive model for estimating monthly ecosystem evapotranspiration. Ecohydrology, 4(2), 245-255. DOI 10.1002/eco.194

Taiz, L., Zeiger, E., Møller, I.M., Murphy, A. 2015. Plant physiology and development.

Tautz, H. 1971. Wärmeleitung und Temperaturausgleich: die mathematische Behandlung instationärer Wärmeleitungsprobleme mit Hilfe von Laplace-Transformationen. : Verlag Chemie.

Wang, S., Trishchenko, A.P., Khlopenkov, K.V., Davidson, A. 2006. Comparison of International Panel on Climate Change Fourth Assessment Report climate model simulations of surface albedo with satellite products over northern latitudes. Journal of Geophysical Research: Atmospheres, 111(D21).

Zeppel, M.J.B., Macinnis-Ng, C.M.O., Yunusa, I.A.M., Whitley, R. J., Eamus, D. 2008. Long term trends of stand transpiration in a remnant forest during wet and dry years. Journal of Hydrology, 349(1-2), 200-213. DOI 10.1016/j.jhydrol.2007.11.001

Zürcher, E., Cantiani, M.G., Guerri, F.S., Michel, D. 1998. Tree stem diameters fluctuate with tide. Nature, 392(6677), 665-666.